

The removal of Basic Blue 3 from aqueous solutions by chitosan-based adsorbent: Batch studies

Grégorio Crini^{a,*}, Frédéric Gimbert^a, Capucine Robert^a, Bernard Martel^b, Olivier Adam^a,
Nadia Morin-Crini^a, François De Giorgi^a, Pierre-Marie Badot^a

^a Université de Franche-Comté, Laboratoire de Biologie Environnementale, EA 3184 USC INRA, 25000 Besançon, France

^b Université des Sciences et Technologies de Lille, Laboratoire de Chimie Organique et Macromoléculaire,
UMR 8009, 59655 Villeneuve d'Ascq, France

Received 27 July 2006; received in revised form 9 August 2007; accepted 10 August 2007

Available online 15 August 2007

Abstract

Chitosan-based adsorbent (CHITOD material) is used for the removal of Basic Blue 3 (BB 3) from aqueous solutions. The adsorption of BB 3 on CHITOD material was studied as a function of time, sorbent mass and concentration. The influence of these parameters on the adsorption capacity was evaluated using the batch method. Results of adsorption experiments and kinetic data showed that (i) the CHITOD adsorbent exhibited high sorption capacities toward BB 3; (ii) the Langmuir equation represented the best fit of experimental data; (iii) the dye sorption on material was exothermic and spontaneous in nature; (iv) the kinetic measurements showed that the process was rapid; (v) the adsorption kinetics followed a pseudo-second order model; and (vi) the sorption was dependent on the presence of sulfonate groups. Non-linear method was also found to be more appropriate method for estimating the isotherm and kinetic parameters.

© 2007 Elsevier B.V. All rights reserved.

Keywords: Chitosan; Adsorbent; Adsorption; Basic Blue 3; Cationic dye; Batch method; Kinetic and isotherm models; Correlation coefficient; Chi-square

1. Introduction

Chitosan, a linear copolymer composed of (1–4)-linked D-glucosamine and N-acetyl-D-glucosamine, is a polysaccharide prepared by N-deacetylation of chitin (second abundant polymer in nature after cellulose) [1]. Chitin is obtained from the exoskeleton of crustaceans, the cuticles of insects and the cell walls of fungi. However, chitin and chitosan are only commercially extracted from crustaceans (crab, krill, crayfish) primarily because a large amount of the crustacean's exoskeleton is available as a by-product of food processing.

As a functional biological polymer, chitosan offers an interesting set of characteristics, including non-toxicity, biodegradability, biocompatibility, bioadhesivity, and bioactivity. This material also presents economical advantages (in many countries fishery wastes are low-cost sources and suitable for producing chitosan) and exhibits remarkable physicochemical

properties such as an hydrophilic character, a sufficient flexibility of the linear chain, an easy chemical derivatization, a capability to interact and to adsorb various substrates, and cationic properties which are unique among abundant polysaccharides.

Chitosan and its derivatives exhibit innumerable applications in a wide range of fields such as food [2,3], pharmacy [4–6], biomedicine [7–9], cosmetics [10], biotechnology [10,11] and agriculture [10,12]. These versatile materials are also widely applied in the textile, pulp and paper industries [10], and in clarification and water purification [13–24] as coagulating [13,14], flocculating [15,16], chelating [10,17,18] and complexing agents [10,17,18]. Different reviews have recently been reported for wastewater treatment purposes, including metal complexation [19,20], dye removal [21], complexing adsorbent matrices [22,23], and membranes [24].

As already mentioned, chitosan has widely been studied for pollutant adsorption from aqueous solutions: the cationic character, along with the presence of reactive functional groups in polymer chains, has given it particular possibilities as efficient adsorbent agents. It is evident from the abundant literature data

* Corresponding author. Tel.: +33 3 81 66 65 64; fax: +33 3 81 66 64 38.
E-mail address: gregorio.crini@univ-fcomte.fr (G. Crini).

Nomenclature

a_L	Langmuir isotherm constant (l/mg)
A	Temkin isotherm constant (l/g)
B	Temkin isotherm constant
C_e	liquid phase dye concentration at equilibrium (mg/l)
C_0	initial dye concentration in liquid phase (mg/l)
k_1	equilibrium rate constant of pseudo-first order sorption (min^{-1})
k_2	equilibrium rate constant of pseudo-second order sorption (g/mg min)
k_i	intraparticle diffusion rate constant ($\text{mg/g min}^{-1/2}$)
K	saturation constant (mg/l)
K_F	Freundlich constant (l/g)
K_L	Langmuir isotherm constant (l/g)
m	mass of adsorbent used (g)
n	cooperative binding constant
n_F	Freundlich isotherm exponent
q_e	amount of dye adsorbed at equilibrium (mg/g)
q_{max}	maximum adsorption capacity of the adsorbent (mg/g)
q_t	amount of dye adsorbed at time t (mg/g)
r^2	non-linear correlation coefficient
R^2	linear correlation coefficient
t	time (min)
t_e	equilibrium time (min)
V	volume of dye solution (l)
x	amount of dye adsorbed (mg)
<i>Greek symbols</i>	
α	initial adsorption rate (mg/g min)
β	Elovich desorption constant (g/mg)
χ^2	Chi-square test statistic

that this biomaterial offers a great potential in the adsorption field and might be a promising adsorbent for environmental purpose [19–22]. In particular, one of the major applications is based on its ability to bind strongly heavy and toxic metals. It represents an attractive alternative to other conventional com-

mercial adsorbents because of its low cost and local availability, high reactivity, excellent chelation behavior and high selectivity towards heavy metals [17,19,20].

Chitosan is also known as an effective adsorbent for proteins [25], saccharides [26], drugs [27], oils [28], bacterial suspensions [29], phenolic derivatives [17,30,31], and also for dye wastewater removal [10,21]. In recent years, numerous studies on chitosan-based biomaterials for dye removal demonstrated that these versatile biosorbents are efficient and have a high affinity for many classes of dyes [32–47], including acid, direct, mordant, reactive and disperse dyes (Table 1). However, only a limited number of published studies can be found on the use of chitosan as an adsorbent for cationic (basic) dye removal.

In this paper, we propose chemical grafting of sulfonate groups onto chitosan as a means to confer the ability to adsorb basic dyes, in particular Basic Blue 3 (BB 3). Several adsorption and kinetic studies are presented and discussed here. The equilibrium data were analyzed using Freundlich, Langmuir, Temkin and Generalized isotherms. In order to investigate the mechanism of sorption, adsorption data were modeled using the pseudo-second order kinetic equation, Elovich equation and intraparticle diffusion model. The characteristics parameters for each model were determined. A comparison was made between the linear and non-linear methods of estimating isotherm and kinetic parameters.

2. Experimental

2.1. Adsorbents

Two chitosan-based sorbents, namely CHITO and CHITOD, were used in this study. Their characteristics are reported in Table 2. CHITO (prepared from crab shells, degree of acetylation = 20%) was supplied by Protan (USA). CHITOD was prepared in one step by reacting chitosan with 4-formyl-1,3-benzene sodium disulfonate in the presence of sodium cyanoborohydride (Fig. 1). The synthesis of CHITOD has already been described in detail in previous works [48,49].

2.2. Dye

The sorption capacity was investigated using C.I. Basic Blue 3 (BB 3, Classification Number 51004; chemical class monox-

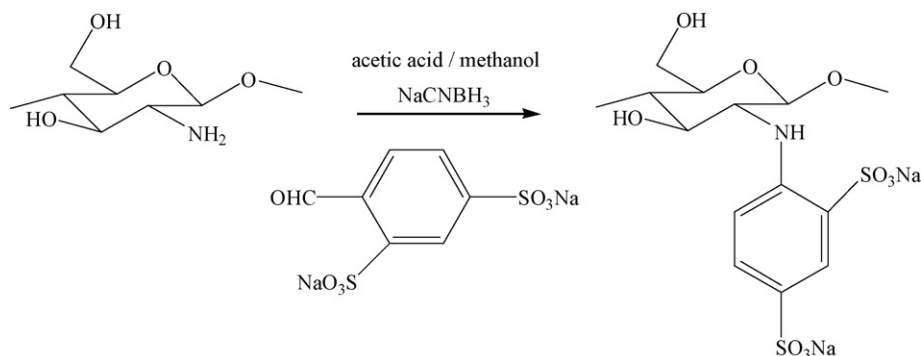


Fig. 1. Synthesis of CHITOD.

Table 1
Recent research on dye capture by chitosan-based adsorbents (selected papers)

Dye investigated	Classification	Chemical type	q_{\max}^a	Reference
Acid black 1	Anionic	Diazo	800 ^b	[38]
Acid blue 113	Anionic	Diazo	250 ^b	[38]
Acid orange 7	Anionic	Monoazo	1940	[35]
Acid orange 10	Anionic	Monoazo	922.9	[36]
Acid orange 12	Anionic	Monoazo	1883	[33]
Acid orange 12	Anionic	Monoazo	1954	[35]
Acid orange 12	Anionic	Monoazo	973.3	[36]
Acid green 25	Anionic	Anthraquinone	1471	[33]
Acid green 25	Anionic	Anthraquinone	645.1	[36]
Acid green 25	Anionic	Anthraquinone	525	[37]
Acid green 25	Anionic	Anthraquinone	850 ^b	[38]
Acid red 14	Anionic	Monoazo	1940	[35]
Acid red 18	Anionic	Monoazo	693.2	[36]
Acid red 73	Anionic	Diazo	728.2	[36]
Acid violet 5	Anionic	Monoazo	160 ^b	[38]
Acid yellow 25	Anionic	Monoazo	220 ^b	[38]
Metanil yellow	Anionic	Monoazo	1334	[32]
Direct blue 14	Anionic	Diazo	90 ^b	[38]
Direct red 81	Anionic	Diazo	2383	[35]
Direct yellow 4	Anionic	Diazo	620	[38]
Mordant blue 29	Anionic	Triphenylmethane	420 ^b	[38]
Mordant brown 33	Anionic	Monoazo	2000 ^b	[38]
Mordant orange 10	Anionic	Diazo	1600 ^b	[38]
Reactive black 5	Anionic	Diazo	440 ^b	[38]
Reactive black 5	Anionic	Diazo	750–1000 ^b	[44]
Reactive blue 2	Anionic	Anthraquinone	2498	[35]
Reactive red 2	Anionic	Monoazo	2422	[35]
Reactive red 141	Anionic	Diazo	67.9	[46]
Reactive yellow 2	Anionic	Monoazo	2436	[35]
Reactive yellow 86	Anionic	Monoazo	1911	[35]
Basic Blue 9	Cationic	Thiazine	330 ^b	[43]
Basic violet 3	Cationic	Triphenyl methane	1546 ^b	[40]

^a q_{\max} : monolayer adsorption capacity in mg/g.

^b In $\mu\text{mol/g}$.

Table 2
Characteristics of chitosan-based adsorbents

Adsorbents	Source	Type	BET ^a	SO ₃ ⁻ content ^b	DS ^c
CHITO	Crab	Bead	18	0	
CHITOD	Crab	Powder	25	3.1	83

^a Specific surface areas, in m²/g.

^b In meq/g, from potentiometric method.

^c Degree of substitution in %, from NMR data.

azine; MW 359.9 g/mol) as model guest solute. This cationic dye was commercial product and used without purification (see Fig. 2 for the structural formulae). An accurately weighted quantity of the dye was dissolved in double-distilled water to prepare stock solution (200 mg/l). Experimental solutions of

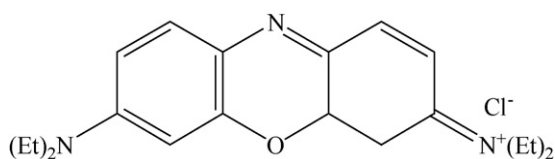


Fig. 2. Chemical structure of C.I. 51004 Basic Blue 3 (BB 3, chemical class: monoxazine).

the desired concentrations were obtained by successive dilutions. The calculated concentrations take into account the dye purity. Dye concentration in solutions was determined spectrophotometrically using a UV/vis Uvikon spectrophotometer (UVK-Lab-Serlabo, France). The dye solution was initially calibrated for concentration in terms of absorbance unit.

2.3. Sorption of BB 3 by batch technique

Adsorption isotherms and kinetics were determined by the batch method. In each experiment, a fixed mass of chitosan was mixed with 20 ml of a NaCl 0.1 mol/l aqueous solution of BB 3 at a known concentration in a tightly closed flask. The initial pH of the solution was adjusted to 3.0 ± 0.1 . The solution was then stirred on a rotating shaker at $25 \text{ }^\circ\text{C} \pm 1 \text{ }^\circ\text{C}$. Initial pollutant concentration in the solution was varied to investigate its effect on the adsorption capacity. Studies were also conducted for various time intervals to determine when adsorption equilibrium was reached. The dye concentration of the supernatant was determined by spectrophotometry at 654 nm. Before measurement of the dye concentration, the mixture was filtered through a membrane filter. Blanks were run without any adsorbent to determine the extent of dye removal by filter.

2.4. Error analysis

In the single-component isotherm studies, the optimization procedure requires an error function to be defined in order to quantitatively compare the applicability of different models in fitting to data. To determine isotherm constants for two-parameter isotherms, two methods are available: fitting the isotherm equation to the data in its non-linear form or converting the equation in a linear form by transforming the isotherm variables. In this study, both linear and non-linear coefficients of determination were determined. Moreover, as it is also necessary to analyze the data set to confirm the best-fit isotherm for the sorption system, the Chi-square test was used. The Chi-square test statistic (χ^2) is basically the sum of the squares of the differences between the experimental data and data obtained by calculating from models, with each squared difference divided by the corresponding data obtained by calculating from models. The values were calculated for the non-linear models but also for their linearized forms, using back-transformation of the calculated data to allow both forms to be compared. If modeled data are similar to the experimental data, χ^2 will be a small number; if they are different, χ^2 will be a large number.

3. Results and discussion

3.1. Adsorption of BB 3 on chitosan-based adsorbents

Fig. 3 shows the sorption capacity (expressed in percentage uptake, R in %) of Basic Blue 3 (BB 3) on two chitosan-based adsorbents, raw chitosan (CHITO) and modified chitosan (CHITOD), respectively without and with sulfonate groups. Preliminary kinetic experiments had shown that 40 min contact time was sufficient for reaching sorption equilibrium. The experiments were performed in triplicate under identical conditions and were found reproducible (experimental error within 3%). R was calculated from:

$$R = \frac{100(C_0 - C_e)}{C_0}$$

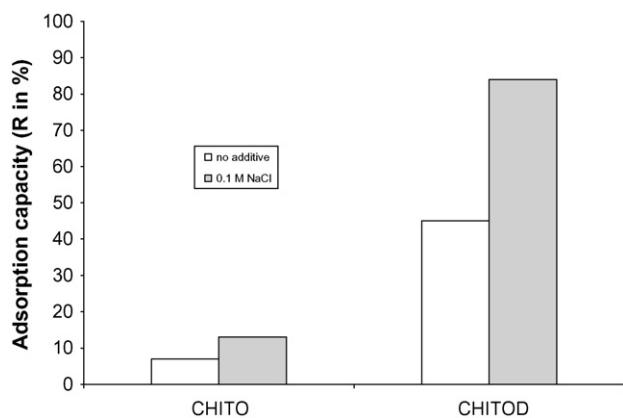


Fig. 3. Comparison between adsorption capacity (R in %) of BB 3 on raw chitosan (CHITO) and modified chitosan (CHITOD) (conditions: dye concentration = 40 mg/l; contact time = 40 min; NaCl concentration = 0.1 mol/l; pH 6.5).

where C_0 and C_e are the initial and equilibrium concentrations of BB 3 in solution (mg/l), respectively.

As expected, BB 3 did not interact with raw chitosan ($R = 7\%$) at pH 6.5. The sorption capacity was very low due to weak electrostatic interactions between the dye and polymer. As a matter of fact, BB 3 is a basic dye containing cationic functions (see Fig. 2) and chitosan presents a certain neutrality in the experimental pH conditions. For CHITOD, which contained sulfonate groups, an increase of the sorption capacity was observed ($R = 45\%$). As described in Table 2, no drastic changes in the specific surface area values of the samples were observed, suggesting that the differences in the capacities of the CHITOD sample were mainly due to its sulfonate groups content. This result clearly demonstrated that these groups contributed to the sorption mechanism through electrostatic interactions between SO_3^- groups of the sorbent (which are known as strong cation exchangers) and the cationic sites of BB 3. Fig. 3 also shows the influence of the presence of NaCl on the adsorption capacity. Addition of NaCl produced an important increase of the performance of the adsorbent ($R = 84\%$). This showed that the sorption capacities depended on the ionic strength of the solution. Elsewhere, NaCl is currently used in textile dyeing processes as it promotes the sorption of the dyes by the fibers.

3.2. Equilibrium studies

3.2.1. Influence of the initial dye concentration on adsorption capacity

The dye concentration at equilibrium (q_e in mg/g) was plotted against equilibrium concentration (C_e in mg/l) (Fig. 4). This figure shows the relationship between the amount of BB 3 adsorbed per mass unit of chitosan and its final concentration in the solution. The quantity of sorbent was kept constant. q_e (in mg/g) was

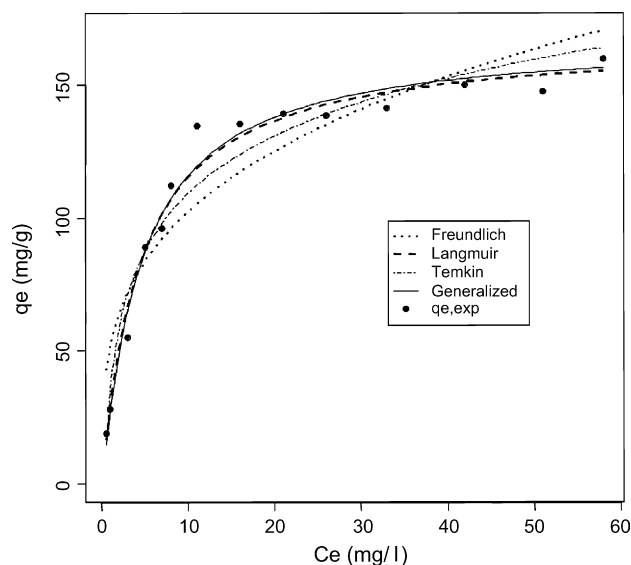


Fig. 4. Adsorption isotherm for BB 3 by CHITOD adsorbent: experimental data and comparison of four isotherm models (conditions: sorbent = 40 mg; contact time = 40 min; NaCl concentration = 0.1 mol/l; pH 3; temperature = 25 °C).

calculated using the following relationships:

$$q_e = \frac{V(C_0 - C_e)}{m}$$

where C_0 and C_e are the initial and equilibrium concentrations of dye in solution (mg/l), respectively; V is the volume of dye solution used (l); and m is the mass of sorbent used (g).

Fig. 4 clearly indicates that the sorption capacity initially strongly increases with the initial concentration in BB 3 and then tends to a plateau. This is due to the saturation of the sorption sites on the adsorbents.

3.2.2. Adsorption equilibrium models

In order to optimize the design of an adsorption system to remove dye from solutions, it is important to establish the most appropriate correlation for the equilibrium curve. Adsorption equilibrium is established when the amount of dye being adsorbed onto the adsorbent is equal to the amount being desorbed. It is possible to depict the equilibrium adsorption isotherms by plotting the concentration of the dye in the solid phase versus that in the liquid phase. Several isotherms models can be used to describe the equilibrium of adsorption. Four common isotherm equations were tested in the present study: Langmuir [50,51], Freundlich [52], Temkin [53] and Generalized models [54]. These equations are given below:

$$\text{Langmuir : } \frac{C_e}{q_e} = \frac{1}{K_L} + \frac{a_L}{K_L} C_e \quad (1)$$

$$\text{Freundlich : } \ln q_e = \ln K_F + \frac{1}{n_F} \ln C_e \quad (2)$$

$$\text{Temkin : } q_e = B \ln A + B \ln C_e \quad (3)$$

$$\text{Generalized : } \ln \left[\frac{q_{\max}}{q_e} - 1 \right] = \ln K - n \ln C_e \quad (4)$$

In Eq. (1), C_e (mg/l) and q_e (mg/g) are the liquid phase concentration and solid phase concentration of an adsorbate at equilibrium, respectively; K_L (l/g) and a_L (l/mg) are the Langmuir isotherm constants. By plotting C_e/q_e against C_e , it is possible to obtain the value of K_L from the intercept which is $1/K_L$ and the value of a_L from the slope, which is a_L/K_L . q_{\max} (mg/g) is the maximum adsorption capacity of the adsorbent and is numerically equal to K_L/a_L . q_{\max} is a constant related to the area occupied by a monolayer of adsorbate, reflecting the limiting adsorption capacity. In Eq. (2), K_F is a constant (l/g) for the system, related to the bonding energy. The Freundlich constant can be defined as an adsorption or distribution coefficient and represents the quantity of dye adsorbed onto an adsorbent for an equilibrium concentration unit. $1/n_F$ (heterogeneity factor, ranging between 0 and 1) is a measure for the adsorption intensity or surface heterogeneity. A plot of $\ln q_e$ versus $\ln C_e$ enables the empirical constants K_F and $1/n_F$ to be determined from the intercept and slope of the linear regression, respectively. In Eq. (3), A and B are the Temkin isotherm constants. The constant B is related to the heat of adsorption. A plot of q_e versus $\ln C_e$ enables one to determine the constants A and B . In Eq. (4), q_e and C_e are as defined in Eq. (2); K is the saturation constant (mg/l) and n is the cooperative binding constant. q_{\max} is the theoretical monolayer capacity (as defined in Eq. (1)). A plot of the equilibrium data in form of $\ln[(q_{\max}/q_e) - 1]$ versus $\ln C_e$ gives K and n constants. Applicability of the isotherm equations was compared by judging the correlation coefficients.

Fig. 5 shows a comparison of adsorption isotherms for curve fitting of the experimental results with above four adsorption

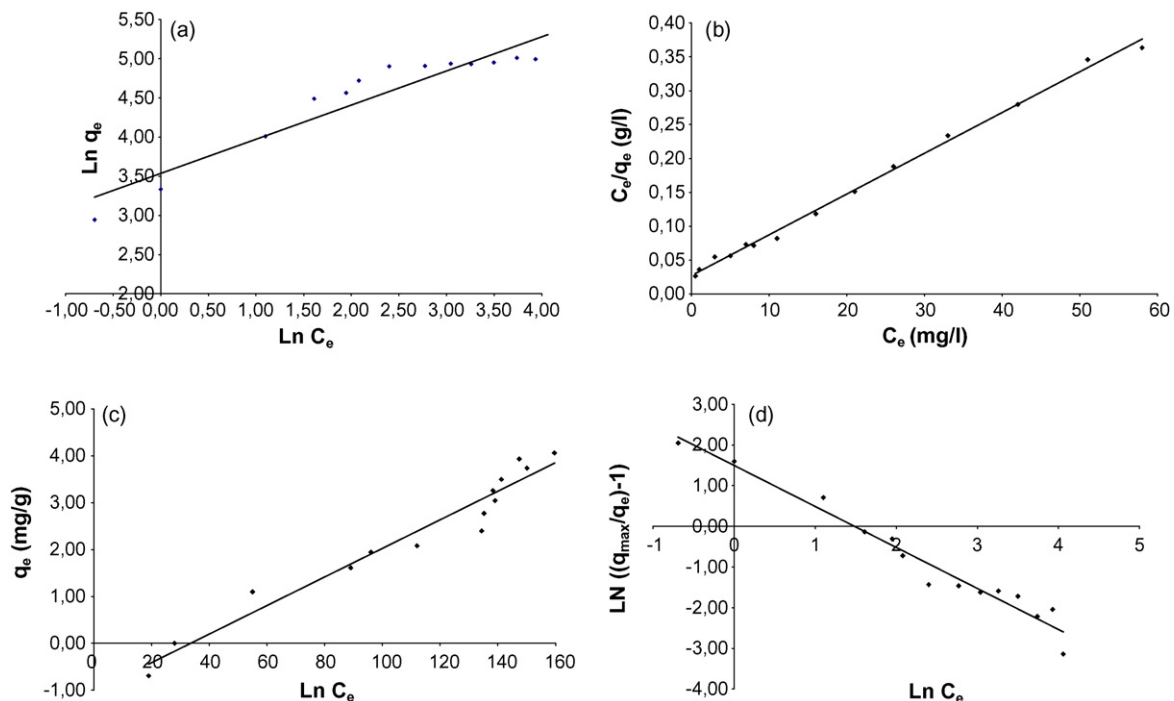


Fig. 5. Adsorption isotherms for Basic Blue 3 by CHITOD adsorbent (a) Freundlich isotherm; (b) Langmuir isotherm; (c) Temkin isotherm; and (d) Generalized isotherm.

Table 3

Summary of the isotherm constants, and comparison of linear (R^2) and non-linear (r^2) correlation coefficients and the Chi-square test statistics (χ^2) for different isotherm models

Isotherm	Linear form			Non-linear form		
	Parameters	R^2	χ^2	Parameters	r^2	χ^2
Freundlich	$K_F = 34.28$ (l/g) $n_F = 2.29$	0.8982	62.3484	$K_F = 52.41$ (l/g) $n_F = 3.44$	0.8738	46.6598
Langmuir	$K_L = 37.03$ (l/g) $a_L = 0.222$ (l/mg) $q_{\max} = 166.5$ (mg/g)	0.9965	6.2125	$K_L = 36.99$ (l/g) $a_L = 0.221$ (l/mg) $q_{\max} = 167.4$ (mg/g)	0.9787	6.1897
Temkin	$A = 3.30$ (l/g) $B = 31.23$	0.9512	15.0866	$A = 3.29$ (l/g) $B = 31.23$	0.9512	15.0812
Generalized	$K = 4.47$ (mg/l) $n = 1.01$	0.9624	7.2147	$K = 4.99$ (mg/l) $n = 1.05$	0.9793	6.3741

isotherms. The model parameters from all isotherms obtained are presented in Table 3. Obviously, it can be seen in Fig. 5 that the Langmuir model was found to represent the equilibrium data with a much better fit as compared to the others models tested. On the basis of R^2 values, the experimental data were also correlated reasonably well by the Langmuir adsorption isotherm (the fit is well for the adsorption system under the concentration range studied). The Freundlich equation represented the poorest fit of experimental data than the other equations although the value of $n_F > 1$ reflects the favorable adsorption (Table 3). The Freundlich model is an empirical equation employed to describe heterogeneous systems and multilayer sites. The Temkin model also takes into account the presence of indirect dye/adsorbent interactions.

The fact that the Langmuir isotherm fits the experimental data very well may be due to homogeneous distribution of active sites on the material, since the Langmuir model assumes that the surface is homogeneous. This model is also based on monolayer, uniform and finite adsorption site assumptions, and there is no interaction between molecules adsorbed on neighbouring sites. It is also noted in Table 3 that the monolayer adsorption capacity (i.e., $q_{\max} = 166.5$ mg/g) is significantly important: this adsorbent exhibited high sorption capacities toward cationic dye. A direct comparison of literature data using different chitosan-based materials is not possible since both adsorbents, dyes and experimental conditions are not the same. However, it was observed that the q_{\max} of the modified chitosan was comparable to those of the other available materials for cationic dye removal [21].

The free energy change (ΔG) for adsorption at 25 °C was calculated using the following equation:

$$\Delta G = -RT \ln K_L \quad (5)$$

where R is the gas constant (8.314 kJ/mol K); T is the temperature and K_L is the Langmuir constant. The calculated ΔG value was found to be -6.4 kJ/mol. The negative value of free energy change indicated the spontaneous nature of adsorption and confirmed the affinity of CHITOD material for BB 3.

3.2.3. Selection by error analysis

The equilibrium isotherm is an invaluable tool for the analysis and design of adsorption systems and also for the theoretical evaluation and interpretation of thermodynamic parameters. An isotherm may fit experimental data accurately under one set of conditions but fail entirely under another. No single model has been found to be generally applicable [55]. This is readily understandable in the light of the assumptions associated with their respective deviations. For example, the use of R^2 is limited to solving linear forms of isotherm equation which measure the difference between experimental data and theoretical data in linear plots only, but not the errors in isotherm curves. However, linear regression is the most commonly used technique to estimate the sorption. Recently, several studies showed that the linearization of a non-linear isotherm expression produces different outcomes. Wong et al. [36] showed that the values of the individual isotherm constants changed with the error methodology selected. They obtained contradicting results from linearization using different error functions. Similar observations also reported by Allen et al. [55]. Ho et al. [56] showed that linear regression and the non-linear Chi-square analysis gave different models as the best-fitting isotherm for the given data set, thus indicating a significant difference between the analytical methods. They reported that the non-linear Chi-square test provided a better determination for the experimental data.

In this study, both coefficients of correlation and Chi-square test statistics were used for both linear and non-linear forms of the isotherms. Fig. 4 shows the isotherms curves for BB 3 onto CHITOD adsorbent at 25 °C along with the experimental data. The curves were generated using the non-linearized equation of different equilibrium models. The Chi-square test statistic (χ^2) and non-linear coefficient of correlation (r^2) were obtained and are shown in Table 3. Based on χ^2 comparisons between models, it was observed that, in simulation, the equilibrium data were very well represented by the Langmuir isotherm model when compared to the others. There was a good agreement between the experimental values and the calculated values. According to the fitting method (linear or non-linear forms of the model), isotherm parameter estimates might change (Table 3). Accurate calculations of the χ^2 for the linear and the non-linear forms of the models provide qualitative information to compare and

choose the best fitting method. Therefore, in our experimental conditions, the non-linear method appeared as a better way to obtain accurate model parameters for the four isotherms tested (Table 3). These results match up with those of Vasanth Kumar and Sivasenan [57] who recently showed the better efficiency of the non-linear method to estimate Langmuir, Freundlich and Redlich–Peterson parameters for basic dyes onto activated carbon.

3.3. Adsorption kinetics

3.3.1. Effect of contact time

The adsorption data of BB 3 versus contact time is presented in Fig. 6. The adsorbate concentration in the solution (q_t in mg/g) was determined at different times from 20 mg/l initial dye solutions and in the presence of 10, 20 and 40 mg of sorbent. All the experiments were realized at pH 3 and at $25\text{ }^\circ\text{C} \pm 1\text{ }^\circ\text{C}$. The plots representing the dye adsorption by chitosan can be split in three distinct regions: the first one indicates the instantaneous sorption of the dye within 4 min of contact time, suggesting rapid external diffusion and surface adsorption; the second one shows a gradual equilibrium and the third one indicates the equilibrium state. The amount of dye adsorbed increased with contact time and this confirmed strong interactions between the dye and the material driven by electrostatic interactions between the cationic dye and the SO_3^- groups of CHITOD. The kinetics of sorption were fast (the equilibrium time, t_e , was found to be 40 min in the three experiments) and was independent from the mass of sorbent present in the batch. Fig. 6 also displays that q_t increased proportionally with regard to the amount of sorbent. q_t increased from 33.5 to 134.5 mg/g as the adsorbent dose was increased from 10 to 40 mg. The plots are single, smooth, and continuous, leading to saturation, suggesting the possible monolayer coverage of dye on the surface of the adsorbent, and this confirms the applicability of the Langmuir model.

3.3.2. Kinetic models

The kinetics of dye adsorption on the sorbent were analyzed using pseudo-second order and Elovich kinetic models. The

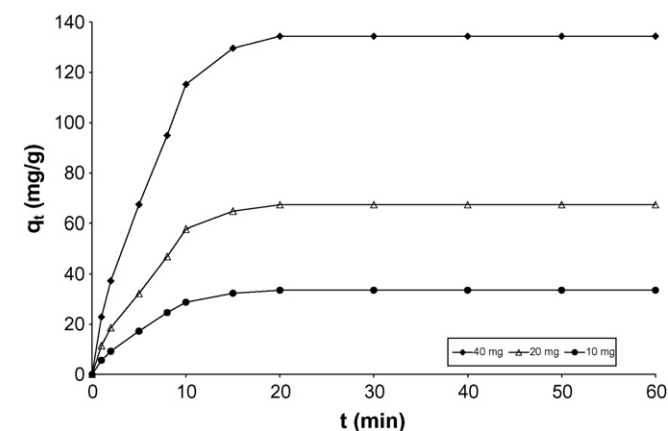


Fig. 6. Kinetics of adsorption capacity of BB 3 by CHITOD adsorbent at three concentrations in the batch (10, 20 and 40 mg) (conditions: dye concentration = 20 mg/l; NaCl concentration = 0.1 mol/l; pH 3; temperature = $25\text{ }^\circ\text{C}$).

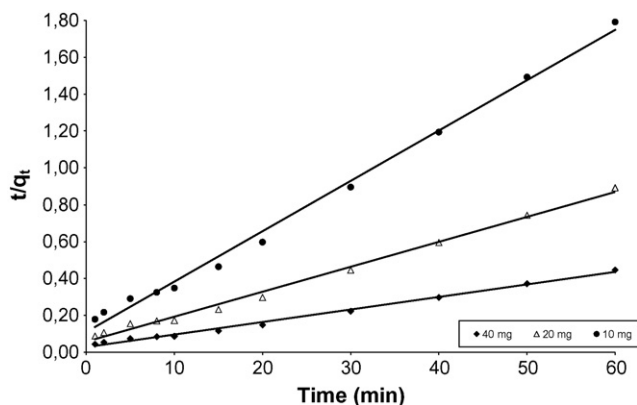


Fig. 7. Pseudo-second order kinetics of BB 3 adsorption onto CHITOD adsorbent at three concentrations in the batch (10, 20 and 40 mg), according to the pseudo-second order kinetic model proposed by Ho and McKay [56,57].

pseudo-second order model proposed by Ho and McKay [58,59] can be represented in the following linear form:

$$\frac{t}{q_t} = \frac{1}{k_2 q_e^2} + \frac{1}{q_e} t \quad (6)$$

where q_t (mg/g) and q_e (mg/g) are the amount of dye adsorbed at time t and equilibrium, respectively; and k_2 is the equilibrium rate constant of pseudo-second order sorption (g/mg min). The parameters k_2 and q_e can be directly obtained from the intercept and slope of the plot of t/q_t against t .

To find the order of the kinetics of adsorption of BB 3, the first-order kinetic equation was tested but no linear correlation was observed. Then, t/q_t versus time graphs were plotted, as shown in Fig. 7. The k_2 and $q_{e,\text{calc}}$ values, computed from Eq. (6) along with calculated correlation coefficients are listed in Table 4. It is clear that the kinetics of dye adsorption on material followed this model, suggesting that chemisorption might be the rate-limiting step that controlled the adsorption process. The plots gave a linear relationship with correlation coefficients were above 0.993. The calculated $q_{e,\text{calc}}$ values agreed with experimental $q_{e,\text{exp}}$ values. These results also showed that the sorption system studied fitted with the pseudo-second order model for the entire sorption period. It was also noted that increasing the sorbent mass four times, the sorption pseudo-second order equilibrium constant rate decreased from 0.00674 to 0.00164. Recently, Azizian [60] reported similar observation.

Table 4
Pseudo-second order kinetic parameters for the adsorption of Basic Blue 3 at various adsorbent dose

Adsorbent dose (mg)	Pseudo-second order model			
	$q_{e,\text{exp}}$ (mg/g)	k_2 (mg/mg min)	$q_{e,\text{cal}}$ (mg/g)	R^2
40	134.4	0.00164	137.1	0.9942
20	67.3	0.00314	70.1	0.9937
10	33.5	0.00674	34.6	0.9949

Conditions: dye concentration = 20 mg/l; NaCl concentration = 0.1 mol/l; temperature = $25\text{ }^\circ\text{C}$; pH 3.

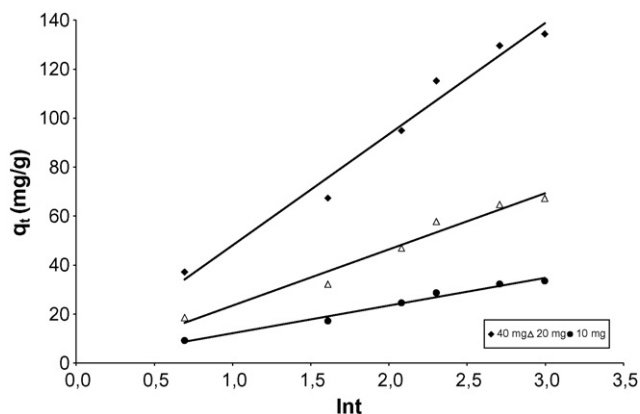


Fig. 8. Plots of Elovich equation for sorption of BB 3 onto CHITOD adsorbent at three concentrations in the batch (10, 20 and 40 mg).

The Elovich model equation [61–63] is generally expressed as:

$$q_t = \frac{\ln \alpha \beta}{\beta} + \frac{1}{\beta} \ln t \quad (7)$$

where α (mg/g min) and β (g/mg) are the initial adsorption rate and the desorption constant, respectively, during any one experiment. If BB 3 adsorption fits the Elovich model, a plot of q_t versus $\ln t$ should yield a linear relationship with a slope of $1/\beta$ and an intercept of $\ln \alpha \beta / \beta$.

Fig. 8 shows that the dye adsorption also fits the Elovich equation. Table 5 lists the kinetic constants obtained from the plots of q_t against $\ln t$. The results showed that the values of initial adsorption rate (α) and desorption constant (β) varied in function of the sorbent amount. Thus on increasing the sorbent quantity from 10 to 40 mg, the value of β increases from 0.022 to 0.088 g/mg.

3.3.3. Intraparticle diffusion model

In a batch system under rapid stirring, there is a possibility that the transport of the adsorbate from the solution into the bulk of the adsorbent is the rate-controlling step. This possibility was tested in terms of a graphical relationship between the amount of dye adsorbed and the square root of time. According to the intraparticle diffusion model proposed by Weber and Morris [64], the initial rate of intraparticle diffusion is given by the equation:

$$q_t = k_i t^{1/2} + C \quad (8)$$

where q_t is the amount of dye on the surface of the sorbent at time t (mg/g), k_i is the intraparticle diffusion rate constant

Table 5
Elovich parameters for the adsorption of Basic Blue 3 at various adsorbent dose

Adsorbent dose (mg)	α	β	R^2
40	48.22	0.022	0.9749
20	23.55	0.043	0.9666
10	12.26	0.088	0.9794

Conditions: dye concentration = 20 mg/l; NaCl concentration = 0.1 mol/l; temperature = 25 °C; pH 3.

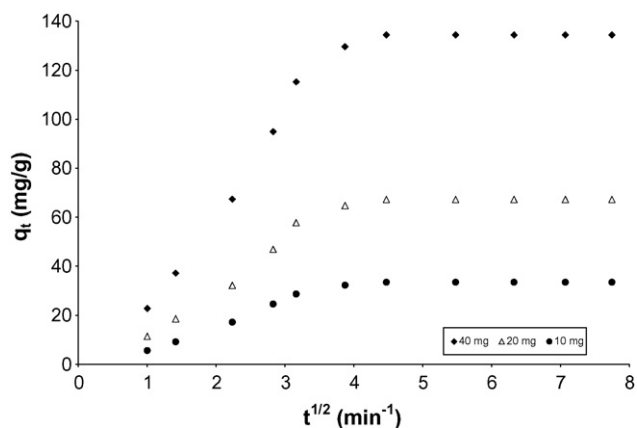


Fig. 9. Amount of dye adsorbed versus $t^{1/2}$ for intraparticle transport of BB 3 by CHITOD adsorbent at three concentrations in the batch (10, 20 and 40 mg), according to the intraparticle diffusion model proposed by Weber and Morris [58].

(mg/g min^{1/2}), t is the time (min) and C is the intercept (mg/g). According to Eq. (8), a plot of q_t versus $t^{1/2}$ should be a straight line when adsorption mechanism follows the intraparticle diffusion process.

The variation of q_t versus $t^{1/2}$ was given in Fig. 9. Values of k_i and correlation coefficient are listed in Table 6, from which it will be seen that the kinetics of the dye sorption on the sorbent follows this model with the correlation coefficients higher than 0.998 for all the three experiments carried out with 10, 20 and 40 mg of sorbent. The results also showed that the sorption process tends to be followed by two phases: the initial curved portion of the plot was due to surface adsorption and rapid external diffusion, indicating a boundary layer effect while the second linear portion was due to intraparticle diffusion. The linear portion of the curves do not pass through the origin suggesting that the mechanism of BB 3 removal on modified chitosan is complex and both the surface adsorption as well as intraparticle diffusion contribute to the adsorption process. Some authors have reported that it is essential for the plots to cross the origin if the intraparticle diffusion is the sole rate-limiting step [32,39,41,45,58,59]. Since this was not the case in this study, it may be concluded that the adsorption of the dye on the modified chitosan was a multi-step process, involving adsorption on the external surface, diffusion into the bulk and chemical reaction (adsorption of dye at an active site via ion-exchange and/or complexation). It was also observed that the intraparticle rate constants (k_i values in Table 6) decreased with increasing sor-

Table 6
Intraparticle diffusion parameters for the adsorption of Basic Blue 3 at various adsorbent dose

Adsorbent dose (mg)	Intraparticle diffusion model	
	k_i (mg/g min ^{-1/2})	R^2
40	1.411	0.9996
20	1.723	0.9989
10	1.935	0.9991

Conditions: dye concentration = 20 mg/l; NaCl concentration = 0.1 mol/l; temperature = 25 °C; pH 3.

Table 7
Comparison of linear (R^2) and non-linear (r^2) correlation coefficients and the Chi-square test statistic (χ^2) for three kinetic models

Adsorbent dose (mg)	Pseudo-second order			Intraparticle diffusion			Elovich model		
	R^2	r^2	χ^2	R^2	r^2	χ^2	R^2	r^2	χ^2
40	0.9942	0.9741	7.7056	0.9996	0.7812	58.0456	0.9749	0.9050	17.0124
20	0.9937	0.9715	4.2196	0.9989	0.7838	28.7063	0.9666	0.9032	8.7611
10	0.9949	0.9751	1.9459	0.9991	0.7752	14.6612	0.9794	0.9033	4.3844

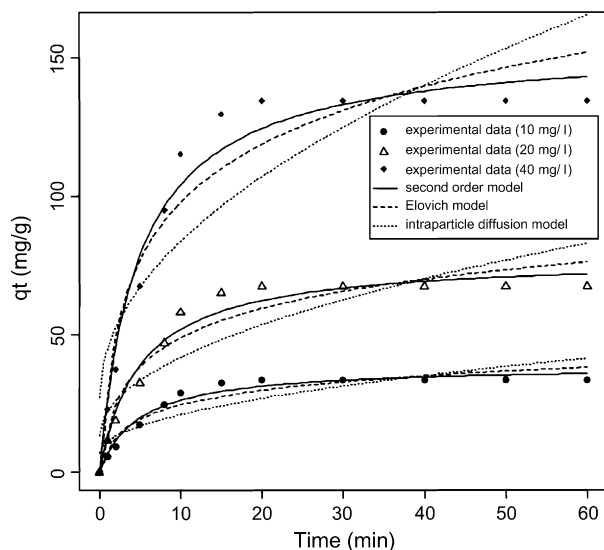


Fig. 10. Comparison between the measured and modeled time profiles for adsorption of BB 3 by CHITOD adsorbent using three different kinetic models.

bent concentration. These values are comparable with some of those reported in the literature [39,45].

Table 7 presents the results of fitting experimental data with pseudo-second order model, intraparticle diffusion model and Elovich kinetic model using linear (R^2) and non-linear (r^2) coefficients of determination, and also the non-linear Chi-square test (χ^2). From this table, the comparison of error analysis showed that the order of deviation was intraparticle diffusion model > Elovich model > pseudo-second order, which indicated that the pseudo-second order model was the best one in describing the adsorption kinetics of dye on material. This was also confirmed in Fig. 10. This figure typically illustrates the comparison between the calculated and measured kinetic results.

4. Conclusions

In this paper, results of adsorption using chitosan-based adsorbent for the removal of Basic Blue 3 from aqueous solutions were presented. This adsorbent exhibited interesting sorption properties toward cationic dye (the maximum adsorption capacity was 166.5 mg/g), depending on the presence of sulfonate groups. The experimental data were examined using four adsorption models and it was found that the Langmuir model represented the best fit of experimental data. Error analysis investigations highlighted the non-linear method as a better way to obtain the isotherm parameters. The nega-

tive value of free energy change indicated the spontaneous nature of adsorption. The kinetic measurements showed that both the process was rapid and followed a pseudo-second order model. The sorption mechanism was a multi-step process, involving adsorption on the external surface, diffusion into the bulk and electrostatic interactions. Works concerning the influence of pH, temperature and dye structure on adsorption are in progress in order to clarify the sorption mechanism and also to show the interest to use these modified chitosans.

Acknowledgements

The authors wish to thank Brigitte Jolibois (LBE, University of Franche-Comté) and Harmel N. Peindy (LCMI, University of Franche-Comté) for assistance during this work; Jozette Duchézeaux (OSEO ANVAR of Franche-Comté) for many helpful discussions; and gratefully acknowledge the financial support of the "Papeterie de Mandeure" (Doubs, Franche-Comté).

References

- [1] J. Synowiecki, N.A. Al-Khateeb, Production, properties, and some new applications of chitin and its derivatives, *Crit. Rev. Food Sci. Nutr.* 43 (2003) 145–171.
- [2] E. Agullo, M.S. Rodriguez, V. Ramos, L. Albertengo, Present and future role of chitin and chitosan in food, *Macromol. Biosci.* 3 (2003) 521–530.
- [3] F. Shahidi, J.K.V. Arachchi, Y.J. Jeon, Food applications of chitin and chitosans, *Trends Food Sci. Technol.* 10 (1999) 37–51.
- [4] M. Prabaharan, J.F. Mano, Chitosan-based particles as controlled drug delivery systems, *Drug Deliv.* 12 (2005) 41–57.
- [5] M.N.V. Ravi Kumar, R.A.A. Muzzarelli, C. Muzzarelli, H. Sashiwa, A.J. Domb, Chitosan chemistry and pharmaceutical perspectives, *Chem. Rev.* 104 (2004) 6017–6084.
- [6] S.A. Agnihotri, N.N. Mallikarjuna, T.M. Aminabhavi, Recent advances on chitosan-based micro- and nanoparticles in drug delivery, *J. Control. Rel.* 100 (2004) 5–28.
- [7] S. Senel, S.J. McClure, Potential applications of chitosan in veterinary medicine, *Adv. Drug Deliv. Rev.* 56 (2004) 1467–1480.
- [8] J. Berger, M. Reist, J.M. Mayer, O. Felt, N.A. Peppas, R. Gurny, Structure and interactions in covalently and ionically crosslinked chitosan hydrogels for biomedical applications, *Eur. J. Pharm. Biopharm.* 57 (2004) 19–34.
- [9] E. Khor, L.Y. Lim, Implantable applications of chitin and chitosan, *Biomaterials* 24 (2003) 2339–2349.
- [10] M.N.V. Ravi Kumar, A review of chitin and chitosan applications, *React. Funct. Polym.* 46 (2000) 1–27.
- [11] B. Krajewska, Applications of chitin- and chitosan-based materials for enzyme immobilizations, *Enzyme Microbiol. Technol.* 35 (2004) 126–139.
- [12] S. Bautista-Banos, A.N. Hernandez-Lauzardo, M.G. Velazquez-del Valle, M. Hernandez-Lopez, E. Ait Barka, E. Bosquez-Molina, C.L. Wilson, Chitosan as a potential natural compound to control pre and postharvest diseases of horticultural commodities, *Crop Protect.* 25 (2006) 108–118.

- [13] B. Meysami, A.B. Kasaeian, Use of coagulants in treatment of olive oil wastewater model solutions by induced air flotation, *Bioresour. Technol.* 96 (2005) 303–307.
- [14] W.P. Cheng, F.H. Chi, R.F. Yu, Y.C. Lee, Using chitosan as a coagulant in recovery of organic matters from the mash and lauter wastewater of brewery, *J. Polym. Environ.* 13 (2005) 383–388.
- [15] G.V. Franks, Stimulant sensitive flocculation and consolidation for improved solid/liquid separation, *J. Colloid Int. Sci.* 292 (2005) 598–603.
- [16] L. Chen, D. Chen, C. Wu, A new approach for the flocculation mechanism of chitosan, *J. Polym. Environ.* 11 (2003) 87–92.
- [17] H.K. No, S.P. Meyers, Application of chitosan for treatment of wastewaters, *Rev. Environ. Contam. Toxicol.* 163 (2000) 1–28.
- [18] M.G. Peter, Application and environmental aspects of chitin and chitosan, *J.M.S. Pure Appl. Chem.* 32 (1995) 629–640.
- [19] E. Guibal, Interactions of metal ions with chitosan-based sorbents: a review, *Sep. Purif. Technol.* 38 (2004) 43–74.
- [20] A.J. Varma, S.V. Deshpande, J.F. Kennedy, Metal complexation by chitosan and its derivatives: a review, *Carbohydr. Polym.* 55 (2004) 77–93.
- [21] G. Crini, Non-conventional low-cost adsorbents for dye removal: a review, *Bioresour. Technol.* 97 (2006) 1061–1085.
- [22] G. Crini, Recent developments in polysaccharide-based materials used as adsorbents in wastewater treatment, *Prog. Polym. Sci.* 30 (2005) 38–70.
- [23] M. Prabaharan, J.F. Mano, Chitosan derivatives bearing cyclodextrin cavities as novel adsorbent matrices, *Carbohydr. Polym.* 63 (2006) 153–166.
- [24] B. Krajewska, Membrane-based processes with use of chitin/chitosan materials, *Sep. Purif. Technol.* 41 (2005) 305–312.
- [25] X. Zeng, E. Ruckenstein, Crosslinked macroporous chitosan anion-exchange membranes for protein separations, *J. Membr. Sci.* 148 (1998) 195–205.
- [26] M. Matsumoto, T. Shimizu, K. Kondo, Selective adsorption of glucose on novel chitosan gel modified by phenylboronate, *Sep. Purif. Technol.* 29 (2002) 229–233.
- [27] F.L. Mi, S.S. Shyu, C.T. Chen, J.Y. Lai, Adsorption of indomethacin onto chemically modified chitosan beads, *Polymer* 43 (2002) 757–765.
- [28] A.L. Ahmad, S. Sumathi, B.H. Hameed, Adsorption of residue oil from palm oil mill effluent using powder and flake chitosan: equilibrium and kinetic studies, *Water Res.* 39 (2005) 2483–2494.
- [29] S.P. Strand, K.M. Varum, K. Ostgaard, Interactions between chitosans and bacterial suspensions: adsorption and flocculation, *Colloids Surf. B: Bioint.* 27 (2003) 71–81.
- [30] S. Zheng, Z. Yang, D.H. Jo, Y.H. Park, Removal of chlorophenols from groundwater by chitosan sorption, *Water Res.* 38 (2004) 2315–2322.
- [31] I. Uzun, F. Güzel, Kinetics and thermodynamics of the adsorption of some dyestuffs and *p*-nitrophenol by chitosan and MCM-chitosan from aqueous solution, *J. Colloid Int. Sci.* 274 (2004) 398–412.
- [32] M.S. Chiou, G.S. Chuang, Competitive adsorption of dye metanil yellow and RB15 in acid solutions on chemically cross-linked chitosan beads, *Chemosphere* 62 (2006) 731–740.
- [33] Y.C. Chang, D.H. Chen, Adsorption kinetics and thermodynamics of acid dyes on a carboxymethylated chitosan-conjugated magnetic nano-adsorbent, *Macromol. Biosci.* 5 (2005) 254–261.
- [34] Y. Shimizu, S. Tanigawa, Y. Saito, T. Nakamura, Synthesis of chemically modified chitosans with a higher fatty acid glycidyl and their adsorption abilities for anionic and cationic dyes, *J. Appl. Polym. Sci.* 96 (2005) 2423–2428.
- [35] M.S. Chiou, P.Y. Ho, H.Y. Li, Adsorption of anionic dye in acid solutions using chemically cross-linked chitosan beads, *Dyes Pigments* 60 (2004) 69–84.
- [36] Y.C. Wong, Y.S. Szeto, W.H. Cheung, G. McKay, Adsorption of acid dye on chitosan—equilibrium isotherm analyses, *Proc. Biochem.* 39 (2004) 693–702.
- [37] G. Gibbs, J.M. Tobin, E. Guibal, Sorption of acid green 25 on chitosan: influence of experimental parameters on uptake kinetics and sorption isotherms, *J. Appl. Polym. Sci.* 90 (2003) 1073–1080.
- [38] E. Guibal, P. McCarrick, J.M. Tobin, Comparison of the sorption of anionic dyes on activated carbon and chitosan derivatives from dilute solutions, *Sep. Sci. Technol.* 38 (2003) 3049–3073.
- [39] I. Uzun, Kinetics of the adsorption of reactive dyes by chitosan, *Dyes Pigments* 70 (2006) 76–83.
- [40] I. Uzun, F. Güzel, Rate studies on the adsorption of some dyestuffs and *p*-nitrophenol by chitosan and monocarboxymethylated(mcm)-chitosan from aqueous solution, *Dyes Pigments* 118 (2005) 141–154.
- [41] A.R. Cestari, E.F.S. Vieira, A.A. Pinto, E.C.N. Lopes, Multiple adsorption of anionic dyes on silica/chitosan hybrid 1. Comparative kinetic data from liquid- and solid-phase models, *J. Colloid Int. Sci.* 292 (2005) 363–372.
- [42] A.R. Cestari, E.F.S. Vieira, A.G.P. dos Santos, J.A. Mota, V.P. de Almeida, Adsorption of anionic dyes on chitosan beads. 1. The influence of the chemical structures of dyes and temperature on the adsorption kinetics, *J. Colloid Int. Sci.* 280 (2004) 380–386.
- [43] M.Y. Chang, R.S. Juang, Adsorption of tannic acid, humic acid, and dyes from water using the composite of chitosan and activated clay, *J. Colloids Int. Sci.* 278 (2004) 18–25.
- [44] G. Gibbs, J.M. Tobin, E. Guibal, Influence of chitosan preprotonation on reactive black 5 sorption isotherms and kinetics, *Ind. Eng. Chem. Res.* 43 (2004) 1–11.
- [45] F.C. Wu, R.L. Tseng, R.S. Juang, Enhanced abilities of highly swollen chitosan beads for color removal and tyrosinase immobilization, *J. Hazard. Mater.* B81 (2001) 167–177.
- [46] N. Sakkayawong, P. Thiravetyan, W. Nakbanpote, Adsorption mechanism of synthetic reactive dye wastewater by chitosan, *J. Colloid Int. Sci.* 286 (2005) 36–42.
- [47] A.C. Chao, S.S. Shyu, Y.C. Lin, F.L. Mi, Enzymatic grafting of carboxyl groups on to chitosan—to confer on chitosan the property of a cationic dye adsorbent, *Bioresour. Technol.* 91 (2004) 157–162.
- [48] G. Crini, G. Torri, M. Guerrini, M. Morcellet, M. Weltrowski, B. Martel, NMR characterization of *N*-benzyl sulfonated derivatives of chitosan, *Carbohydr. Polym.* 33 (1997) 145–151.
- [49] M. Weltrowski, B. Martel, M. Morcellet, Chitosan *N*-benzyl sulfonate derivatives as sorbents for removal of metal ions in an acidic medium, *J. Appl. Polym. Sci.* 59 (1996) 647–654.
- [50] I. Langmuir, The constitution and fundamental properties of solids and liquids, *J.A.C.S.* 38 (1916) 2221–2295.
- [51] I. Langmuir, The adsorption of gases on plane surfaces of glass, mica and platinum, *J.A.C.S.* 40 (1918) 1361–1403.
- [52] H.M.F. Freundlich, Über die adsorption in lösungen, *Zeitschrift für Physikalische Chemie* 57 (1906) 385–471.
- [53] C. Aharoni, D.L. Sparks, Kinetics of soil chemical reactions—a theoretical treatment, in: D.L. Sparks, D.L. Suarez (Eds.), *Rates of Soil Chemical Processes*, Soil Science Society of America, Madison, WI, 1991, pp. 1–18.
- [54] F. Kargi, S. Ozimhici, Biosorption performance of powdered activated sludge for removal of different dyestuffs, *Enzyme Microb. Technol.* 35 (2004) 267–271.
- [55] S.J. Allen, G. McKay, J.F. Porter, Adsorption isotherm models for basic dye adsorption by peat in single and binary component systems, *J. Colloid Int. Sci.* 280 (2004) 322–333.
- [56] Y.S. Ho, W.T. Chiu, C.C. Wang, Regression analysis for the sorption isotherms of basic dyes on sugarcane dust, *Bioresour. Technol.* 96 (2005) 1285–1291.
- [57] K. Vasanth Kumar, S. Sivanesan, Isotherm parameters for basic dyes onto activated carbon: comparison of linear and non-linear method, *J. Hazard. Mater.* B129 (2006) 147–150.
- [58] Y.S. Ho, G. McKay, Kinetic models for the sorption of dye from aqueous solution by wood, *Trans I ChemE* 76 (1998) 183–191.
- [59] Y.S. Ho, G. McKay, A comparison of chemisorption kinetic models applied to pollutant removal on various sorbents, *Trans I ChemE* 76 (1998) 332–340.
- [60] S. Azizian, Kinetic models of sorption: a theoretical analysis, *J. Colloid Int. Sci.* 276 (2004) 47–52.
- [61] S.H. Chien, W.R. Clayton, Application of Elovich equation to the kinetics of phosphate release and sorption in soil, *J. Am. Soil Sci. Soc.* 44 (1980) 265–268.

- [62] E. Demirbas, M. Koby, E. Senturk, T. Ozkan, Adsorption kinetics for the removal of chromium (VI) from aqueous solutions on activated carbons prepared from agricultural wastes, *J. Water SA* 4 (2004) 533–538.
- [63] M.J.D. Low, Kinetic of chemisorption of gases on solids, *Chem. Rev.* 60 (1960) 267–317.
- [64] W.J. Weber, J.C. Morris, Kinetics of adsorption on carbon solution, *J. Sanitary Eng. Div. Am. Soc. Civ. Eng.* 89 (1963) 31–59.